



Crystal structure, Hirshfeld surface analysis and DFT studies of 2-[5-(4-methylbenzyl)-6-oxo-3-phenyl-1,6-dihydropyridazin-1-yl]acetic acid

Said Daoui,^a Cemile Baydere,^{b*} Fouad El Kalai,^{a*} Lhassane Mahi,^c Necmi Dege,^b Khalid Karrouchi^d and Nouredine Benchat^a

Received 6 November 2019

Accepted 13 November 2019

Edited by H. Stoeckli-Evans, University of Neuchâtel, Switzerland

Keywords: crystal structure; hydrogen bonding; DFT; Hirshfeld surface analysis; HOMO–LUMO calculations.

CCDC reference: 1965448

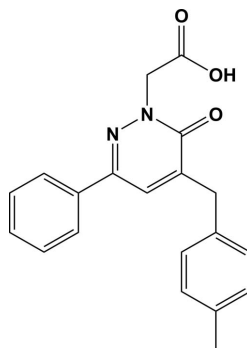
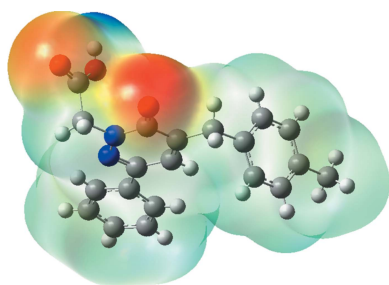
Supporting information: this article has supporting information at journals.iucr.org/e

^aLaboratory of Applied Chemistry and Environment (LCAE), Faculty of Sciences, Mohamed I University, 60000 Oujda, Morocco, ^bDepartment of Physics, Faculty of Arts and Sciences, Ondokuz Mayıs University, 55139-Samsun, Turkey, ^cMoroccan Foundation for Advanced Science, Innovation and Research (Mascir), Department of Nanotechnology, Rabat Design Center, Rue Mohamed Al Jazouli-Madinat Al Irfane, Rabat 10 100, Morocco, and ^dLaboratory of Plant Chemistry, Organic and Bioorganic Synthesis, URAC23, Faculty of Science, B.P. 1014, GEOPAC Research Center, Mohammed V University, Rabat, Morocco. *Correspondence e-mail: cemle28baydere@hotmail.com, fouadelkalai80@gmail.com

The title pyridazinone derivative, C₂₀H₁₈N₂O₃, is not planar. The phenyl ring and the pyridazine ring are inclined to each other by 10.55 (12)°, whereas the 4-methylbenzyl ring is nearly orthogonal to the pyridazine ring, with a dihedral angle of 72.97 (10)°. In the crystal, molecules are linked by pairs of O–H···O hydrogen bonds, forming inversion dimers with an R₂²(14) ring motif. The dimers are linked by C–H···O hydrogen bonds, generating ribbons propagating along the *c*-axis direction. The intermolecular interactions were additionally investigated using Hirshfeld surface analysis and two-dimensional fingerprint plots. They revealed that the most significant contributions to the crystal packing are from H···H (48.4%), H···O/O···H (21.8%) and H···C/C···H (20.4%) contacts. Molecular orbital calculations providing electron-density plots of HOMO and LUMO molecular orbitals and molecular electrostatic potentials (MEP) were also computed, both with the DFT/B3LYP/6–311 G++(d,p) basis set.

1. Chemical context

Pyridazinone derivatives are important biologically active heterocyclic compounds (Dubey *et al.*, 2015; Akhtar *et al.*, 2016), which have been the subject of many studies because of their widespread biological activities, such as inflammatory (Barberot *et al.*, 2018), antibacterial (El-Hashash *et al.*, 2014), antidepressant (Boukharsa *et al.*, 2016), antihypertensive (Demirayak *et al.*, 2004), anti-HIV (Li *et al.*, 2013), anti-convulsant (Partap *et al.*, 2018), and their use as herbicidal agents (Asif, 2013). In addition, it has been shown that pyridazinones are good corrosion inhibitors (Chetouani *et al.*, 2003) and that they can be used as organic extractants of certain metal ions in the aqueous phase (El Kalai *et al.*, 2019b).



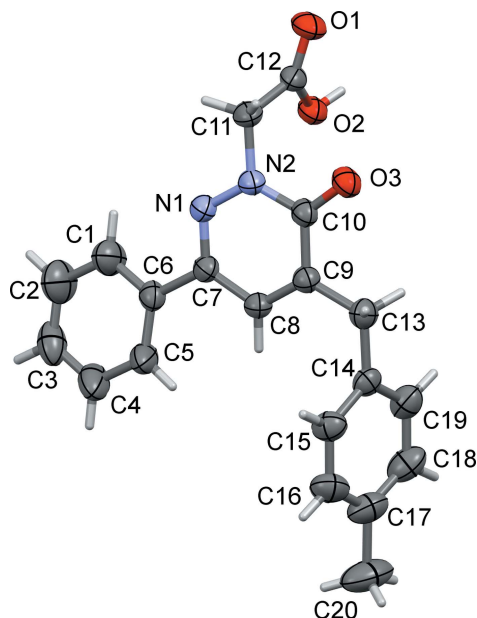


Figure 1
The molecular structure of the title compound, with atom labelling. Displacement ellipsoids are drawn at the 30% probability level.

In a continuation of our investigations of the molecular structures and Hirshfeld surfaces of new pyridazinone derivatives (Daoui *et al.*, 2019*a,b*), we report herein on the synthesis and crystal and molecular structures of the title compound, 2-[5-(4-methylbenzyl)-6-oxo-3-phenyl-1,6-dihydropyridazin-1-yl]acetic acid, as well as the analysis of the Hirshfeld surfaces.

2. Structural commentary

The molecule structure of the title compound is shown in Fig. 1. The phenyl (C1–C6) and pyridazine (C7–C10/N1/N2) rings are twisted relative to each other, making a dihedral

Table 1
Hydrogen-bond geometry (Å, °).

$D-H\cdots A$	$D-H$	$H\cdots A$	$D\cdots A$	$D-H\cdots A$
$O2-H2\cdots O3^i$	0.82	1.83	2.6358 (16)	167
$C3-H3\cdots O1^{ii}$	0.93	2.51	3.430 (3)	172

Symmetry codes: (i) $-x+1, -y+2, -z$; (ii) $x, y, z+1$.

angle of $10.55(12)^\circ$. The 4-methylbenzyl ring (C14–C19) is inclined to the pyridazine ring by $72.97(10)^\circ$. Atoms C9 and C10 of the pyridazine ring show the largest deviations from planarity (r.m.s. deviation = 0.0075 \AA) in positive and negative directions [C10 = $0.0127(11) \text{ \AA}$ and C9 = $-0.0090(11) \text{ \AA}$]. The $O3=C10$ bond length of the pyridazinone carbonyl function is $1.2433(19) \text{ \AA}$ and the N1–N2 bond length in the pyridazine ring is $1.3516(19) \text{ \AA}$, both in accordance with values reported for related pyridazinones (El Kalai *et al.*, 2019*a*; Xu *et al.*, 2005).

3. Supramolecular features

In the crystal, molecules are linked by pairs of $O-H\cdots O$ hydrogen bonds, forming inversion dimers with an $R_2^2(14)$ ring motif (Table 1 and Fig. 2). The dimers are linked by $C-H\cdots O$ hydrogen bonds, forming ribbons that extend along the c -axis direction (Table 1 and Fig. 2). There are no other significant intermolecular interactions present.

4. Database survey

A search of the Cambridge Structural Database (CSD, version 5.40, update August 2019; Groom *et al.*, 2016) using 2-[6-oxopyridazin-1(6*H*)-yl]acetic acid as the main skeleton revealed the presence of six structures similar to the title compound, but with different substituents on the pyridazine ring. Two of these structures are similar to the title compound,

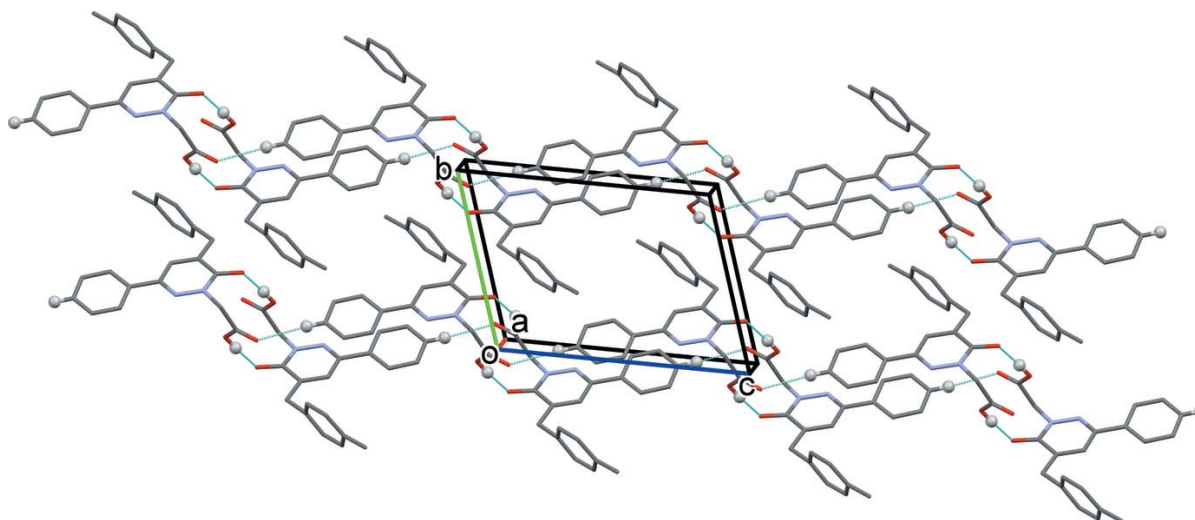


Figure 2
A view along the a axis of the crystal packing of the title compound. The $O-H\cdots O$ and $C-H\cdots O$ hydrogen bonds (see Table 1) are shown as dashed lines. For clarity, only H atoms H2 and H3 (grey balls) have been included.

viz. ethyl {5-[(3-chlorophenyl)methyl]-6-oxo-3-phenylpyridazin-1(6*H*)-yl}acetate (FODQUN; El Kalai *et al.*, 2019*a*) and ethyl 3-methyl-6-oxo-5-[3-(trifluoromethyl)phenyl]-1,6-dihydro-1-pyridazineacetate (QANVOR; Xu *et al.*, 2005).

In FODQUN, the phenyl ring and the pyridazine ring are inclined to each other by 17.41 (13)°, whereas the 3-chlorophenyl ring is nearly orthogonal to the pyridazine ring with a dihedral angle of 88.19 (13)°. In the crystal, C—H···O hydrogen bonds generate inversion dimers with an $R_2^2(10)$ ring motif. The dimers are linked by further C—H···O hydrogen bonds, enclosing $R_2^2(20)$ ring motifs, forming ribbons, similar to the situation in the crystal of the title compound. Weak intermolecular C—H··· π interactions and π – π interactions are also observed in the crystal structure.

In QANVOR, the phenyl and pyridazinone rings are approximately coplanar with a dihedral angle of 4.84 (14)°. In the crystal, inversion-related molecules form dimers through non-classical C—H···O hydrogen bonds. The dimers are linked by a number of C—H···F hydrogen bonds, forming a three-dimensional structure.

5. Hirshfeld surface analysis

Hirshfeld surface analysis was used to quantify the intermolecular contacts of the title compounds, using the software *CrystalExplorer17.5* (Turner *et al.*, 2017). The Hirshfeld surfaces were calculated using a standard (high) surface resolution with the three-dimensional d_{norm} surfaces plotted over a fixed colour scale of –0.7290 (red) to 1.4764 (blue) a.u.. The Hirshfeld surfaces of the title compound were mapped over d_{norm} , shape index and curvedness, and are shown in Fig. 3*a–c*.

The overall two-dimensional fingerprint plot and those delineated into H···H, H···C/C···H, H···O/O···H, H···N/N···H and C···C contacts are illustrated in Fig. 4*a–f*, respectively. The H···H interaction makes the largest contribution (48.4%) to the overall crystal packing. The pair of wings in the fingerprint plot delineated into H···C/C···H contacts, which contribute 20.4% to the Hirshfeld surface, have a nearly symmetrical distribution of points with the tips at $d_e + d_i \sim 2.70$ Å. H···O/O···H contacts make a 21.8% contribution to the Hirshfeld surface. The contacts are

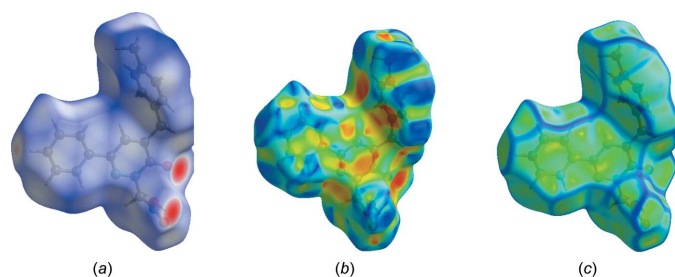


Figure 3
(*a*) The Hirshfeld surface of the title compound mapped over d_{norm} , and plotted in the range –0.7290 to 1.4764 a.u.. (*b*) the Hirshfeld surface mapped over shape-index, (*c*) the Hirshfeld surface mapped over curvedness.

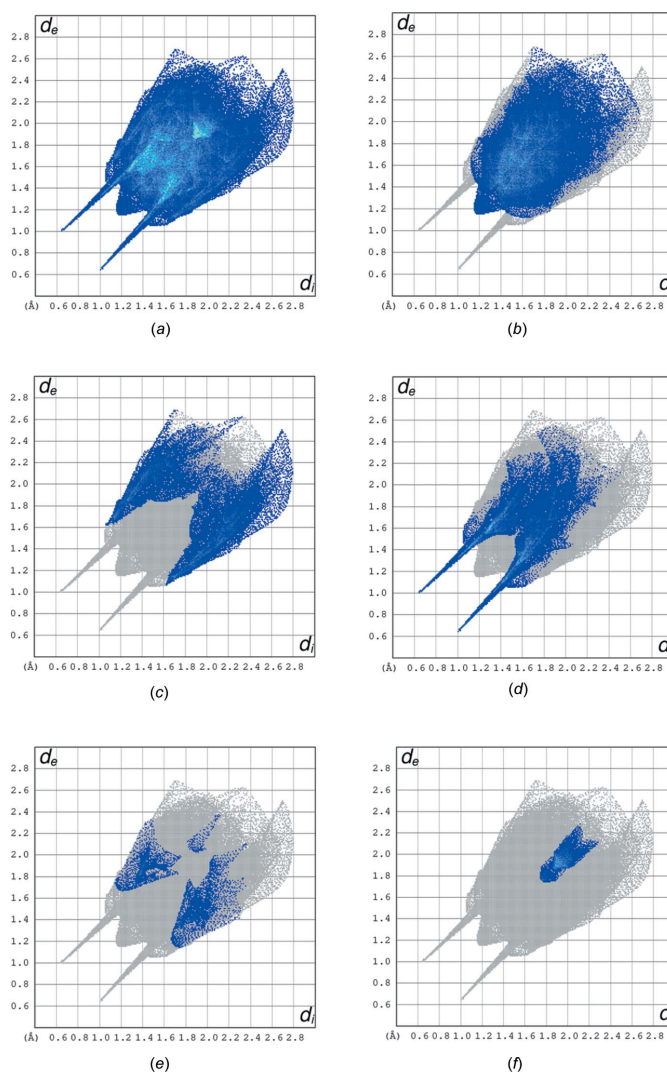


Figure 4
(*a*) The full two-dimensional fingerprint plot for the title compound, and delineated into (*b*) H···H (48.4%), (*c*) H···C/C···H (20.4%), (*d*) H···O/O···H (21.8%), (*e*) H···N/N···H (4.1%) and (*f*) C···C (4.0%) contacts.

represented by a pair of sharp spikes in the region $d_e + d_i \sim 1.64$ Å in the fingerprint plot, Fig. 4*d*. The H···O/O···H contacts arise from intermolecular O—H···O and C—H···O hydrogen bonding (Table 2). The contributions of the other contacts to the Hirshfeld surface are negligible, *i.e.* H···N/N···H of 4.1% and C···C of 4.0%.

6. Frontier molecular orbital analysis

The energy levels for the title compound were computed theoretically *via* density functional theory (DFT) using the standard B3LYP functional and 6–311 G++ (d,p) basis-set calculations (Becke, 1993) as implemented in *GAUSSIAN 09* (Frisch *et al.*, 2009). The HOMO (highest occupied molecular orbital) acts as an electron donor and the LUMO (lowest occupied molecular orbital) as an electron acceptor. When the energy gap is small, the molecule is highly polarizable and has high chemical reactivity. The energy levels, energy gaps,

Table 2

Calculated frontier molecular orbital energies (eV).

FMO	Energy
$E(\text{HOMO})$	-6.4396
$E(\text{LUMO})$	-2.0811
$\Delta E(\text{HOMO-LUMO})$	4.3585
Hardness, η	2.1792
Softness, σ	0.4589
Electronegativity, χ	4.2603

hardness (η), softness (σ) and electronegativity (χ) are given in Table 2. The electron transition from the HOMO to the LUMO energy level is shown in Fig. 5. The chemical hardness and softness of a molecule is a sign of its chemical stability. From the HOMO–LUMO energy gap, we can see whether or not the molecule is hard or soft. If the energy gap is large, the molecule is hard and if small the molecule is soft. Soft molecules are more polarizable than hard ones because they need less energy for excitation. Therefore, from Table 2 we conclude that the title compound can be classified as a hard material with a HOMO–LUMO energy gap of 4.3585 eV.

7. Molecular electrostatic potentials

Molecular electrostatic potential (MEP) displays molecular size and shape as well as positive, negative and neutral electrostatic potential regions in terms of colour grading and is useful in investigating relationships between molecular

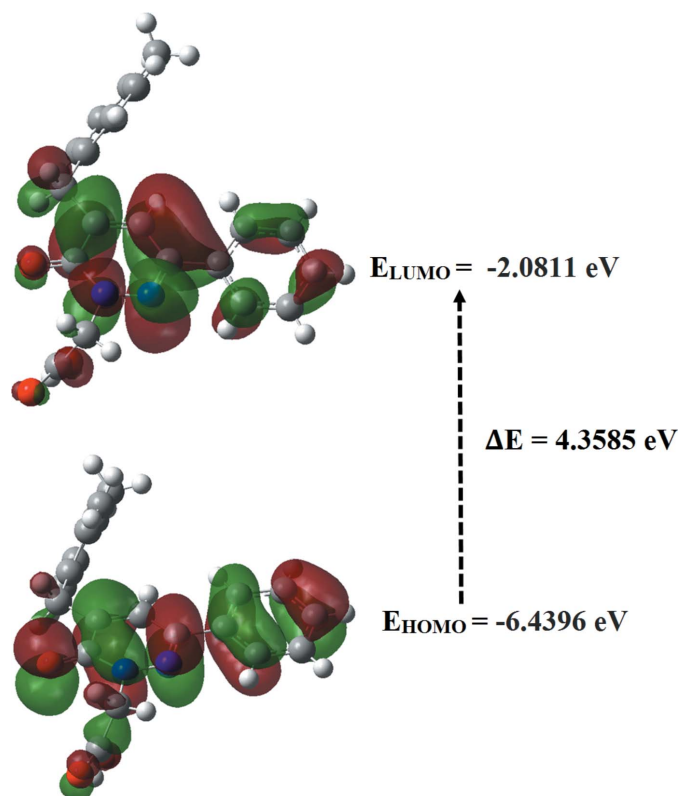


Figure 5
Molecular orbital energy levels of the title compound.

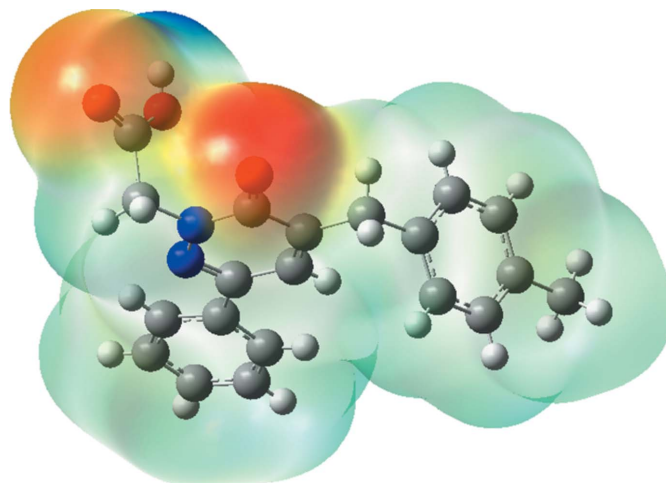


Figure 6
Theoretical molecular electrostatic potential surface for the title compound, calculated using the DFT/B3LYP/6-311 G++ (d,p) basis set.

structure and physicochemical properties (Murray & Sen, 1996; Scrocco & Tomasi, 1978). The MEP map (Fig. 6) was calculated at the B3LYP/6-311 G++ (d,p) level of theory. The red and blue-coloured regions indicate nucleophilic (electron rich) and electrophile regions (electron poor), respectively. The white regions indicate neutral atoms. In the title molecule, the red regions are concentrated at the carbonyl group. It possesses the most negative potential and is thus the strongest repulsion site (electrophilic attack). The blue regions indicate the strongest attraction regions, which are occupied mostly by hydrogen atoms.

8. Synthesis and crystallization

A suspension of ethyl 2-[5-(4-methylbenzyl)-6-oxo-3-phenylpyridazin-1(6*H*)-yl]acetate (3.6 mmol), and 6 *N* NaOH (14.4 mmol) in ethanol (50 ml) was stirred at 353 K for 4 h. The mixture was then concentrated *in vacuo*, diluted with cold water, and acidified with 6 *N* HCl. The final product was filtered off with suction and recrystallized from ethanol. Yellow prismatic crystals were obtained by slow evaporation of the solvent at room temperature.

9. Refinement

Crystal data, data collection and structure refinement details are summarized in Table 3. The hydrogen atoms were fixed geometrically (O–H = 0.82 Å, C–H = 0.93–0.96 Å) and allowed to ride on their parent atoms with $U_{\text{iso}}(\text{H}) = 1.5U_{\text{eq}}(\text{O}, \text{C-methyl})$ and $1.2U_{\text{eq}}(\text{C})$ for other H atoms. For atoms C17–C20, SIMU, DELU and ISOR commands were used (SHELXL; Sheldrick, 2015*b*).

Acknowledgements

The authors acknowledge the Faculty of Arts and Sciences, Ondokuz Mayıs University, Turkey, for the use of the Stoe

IPDS 2 diffractometer (purchased under grant F.279 of the University Research Fund).

References

- Akhtar, W., Shaquiquzzaman, M., Akhter, M., Verma, G., Khan, M. F. & Alam, M. M. (2016). *Eur. J. Med. Chem.* **123**, 256–281.
- Asif, M. (2013). *Mini-Rev. Org. Chem.* **10**, 113–122.
- Barberot, C., Moniot, A., Allart-Simon, I., Malleret, L., Yegorova, T., Laronze-Cochard, M., Bentaher, A., Médebielle, M., Bouillon, J. P., Hénon, E., Sapi, J., Velard, F. & Gérard, S. (2018). *Eur. J. Med. Chem.* **146**, 139–146.
- Becke, A. D. (1993). *J. Chem. Phys.* **98**, 5648–5652.
- Boukharsa, Y., Meddah, B., Tiendrebeogo, R. Y., Ibrahim, A., Taoufik, J., Cherrah, Y., Benomar, A., Faouzi, M. E. A. & Ansar, M. (2016). *Med. Chem. Res.* **25**, 494–500.
- Chetouani, A., Aouniti, A., Hammouti, B., Benchat, N., Benhadda, T. & Kertit, S. (2003). *Corros. Sci.* **45**, 1675–1684.
- Daoui, S., Baydere, C., El Kalai, F., Saddik, R., Dege, N., Karrouchi, K. & Benchat, N. (2019a). *Acta Cryst.* **E75**, 1734–1737.
- Daoui, S., Cinar, E. B., El Kalai, F., Saddik, R., Karrouchi, K., Benchat, N., Baydere, C. & Dege, N. (2019b). *Acta Cryst.* **E75**, 1352–1356.
- Demirayak, S., Karaburun, A. C. & Beis, R. (2004). *Eur. J. Med. Chem.* **39**, 1089–1095.
- Dubey, S. & Bhosle, P. A. (2015). *Med. Chem. Res.* **24**, 3579–3598.
- El-Hashash, M. A., Guirguis, D. B., AbdEl-Wahed, N. A. M. & Kadhim, M. A. (2014). *J. Chem. Eng. Process Technol.* **5**, 1000191–1000196.
- El Kalai, F., Baydere, C., Daoui, S., Saddik, R., Dege, N., Karrouchi, K. & Benchat, N. (2019a). *Acta Cryst.* **E75**, 892–895.
- El Kalai, F., Chelfi, T., Benchat, N., Hacht, B., Bouklah, M., Elaattiaoui, A., Daoui, S., Allali, M., Ben Hadda, T. & Almalki, F. (2019b). *J. Mol. Struct.* **1191**, 24–31.
- Farrugia, L. J. (2012). *J. Appl. Cryst.* **45**, 849–854.
- Frisch, M. J., Trucks, G. W., Schlegel, H. B., Scuseria, G. E., Robb, M. A., Cheeseman, J. R., et al. (2009). *GAUSSIAN09*. Gaussian Inc., Wallingford, CT, USA.
- Groom, C. R., Bruno, I. J., Lightfoot, M. P. & Ward, S. C. (2016). *Acta Cryst.* **B72**, 171–179.
- Li, D., Zhan, P., Liu, H., Pannecouque, C., Balzarini, J., De Clercq, E. & Liu, X. (2013). *Bioorg. Med. Chem.* **21**, 2128–2134.
- Macrae, C. F., Bruno, I. J., Chisholm, J. A., Edgington, P. R., McCabe, P., Pidcock, E., Rodriguez-Monge, L., Taylor, R., van de Streek, J. & Wood, P. A. (2008). *J. Appl. Cryst.* **41**, 466–470.
- Murray, J. S. & Sen, K. (1996). *Molecular Electrostatic Potentials: Concepts and Applications*. Amsterdam: Elsevier.
- Partap, S., Akhtar, M. J., Yar, M. S., Hassan, M. Z. & Siddiqui, A. A. (2018). *Bioorg. Chem.* **77**, 74–83.

Table 3

Experimental details.

Crystal data	
Chemical formula	C ₂₀ H ₁₈ N ₂ O ₃
<i>M_r</i>	334.36
Crystal system, space group	Triclinic, <i>P</i> $\bar{1}$
Temperature (K)	296
<i>a</i> , <i>b</i> , <i>c</i> (Å)	8.4213 (7), 9.0739 (9), 12.2238 (12)
α , β , γ (°)	106.501 (8), 92.390 (8), 100.750 (8)
<i>V</i> (Å ³)	875.43 (15)
<i>Z</i>	2
Radiation type	Mo <i>K</i> α
μ (mm ⁻¹)	0.09
Crystal size (mm)	0.75 × 0.62 × 0.34
Data collection	
Diffractometer	Stoe IPDS 2
Absorption correction	Integration (<i>X-RED32</i> ; Stoe & Cie, 2002)
<i>T_{min}</i> , <i>T_{max}</i>	0.945, 0.959
No. of measured, independent and observed [<i>I</i> > 2 σ (<i>I</i>)] reflections	7687, 3387, 2159
<i>R_{int}</i>	0.029
(<i>sin</i> θ / λ) _{max} (Å ⁻¹)	0.617
Refinement	
<i>R</i> [<i>F</i> ² > 2 σ (<i>F</i> ²)], <i>wR</i> (<i>F</i> ²), <i>S</i>	0.046, 0.130, 1.01
No. of reflections	3387
No. of parameters	228
No. of restraints	33
H-atom treatment	H-atom parameters constrained
$\Delta\rho_{\text{max}}$, $\Delta\rho_{\text{min}}$ (e Å ⁻³)	0.12, -0.14

Computer programs: *X-AREA* and *X-RED32* (Stoe & Cie, 2002), *SHELXT2017* (Sheldrick, 2015a), *SHELXL2018* (Sheldrick, 2015b), *Mercury* (Macrae et al., 2008), *WinGX* (Farrugia, 2012), *PLATON* (Spek, 2009) and *publCIF* (Westrip, 2010).

- Scrocco, E. & Tomasi, J. (1978). *Advances in Quantum Chemistry*. New York: Academic Press.
- Sheldrick, G. M. (2015a). *Acta Cryst.* **A71**, 3–8.
- Sheldrick, G. M. (2015b). *Acta Cryst.* **C71**, 3–8.
- Spek, A. L. (2009). *Acta Cryst.* **D65**, 148–155.
- Stoe & Cie (2002). *X-AREA* and *X-RED32*. Stoe & Cie GmbH, Darmstadt, Germany.
- Turner, M. J., McKinnon, J. J., Wolff, S. K., Grimwood, D. J., Spackman, P. R., Jayatilaka, D. & Spackman, M. A. (2017). *CrystalExplorer17*. University of Western Australia. <http://hirshfeldsurface.net>.
- Westrip, S. P. (2010). *J. Appl. Cryst.* **43**, 920–925.
- Xu, H., Song, H.-B., Yao, C.-S., Zhu, Y.-Q., Hu, F.-Z., Zou, X.-M. & Yang, H.-Z. (2005). *Acta Cryst.* **E61**, o1561–o1563.

supporting information

Acta Cryst. (2019). E75, 1925-1929 [https://doi.org/10.1107/S2056989019015317]

Crystal structure, Hirshfeld surface analysis and DFT studies of 2-[5-(4-methylbenzyl)-6-oxo-3-phenyl-1,6-dihydropyridazin-1-yl]acetic acid

Said Daoui, Cemile Baydere, Fouad El Kalai, Lhassane Mahi, Necmi Dege, Khalid Karrouchi and Nouredine Benchat

Computing details

Data collection: *X-AREA* (Stoe & Cie, 2002); cell refinement: *X-AREA* (Stoe & Cie, 2002); data reduction: *X-RED32* (Stoe & Cie, 2002); program(s) used to solve structure: *SHELXT2017* (Sheldrick, 2015a); program(s) used to refine structure: *SHELXL2018* (Sheldrick, 2015b); molecular graphics: *Mercury* (Macrae *et al.*, 2008) and *PLATON* (Spek, 2009); software used to prepare material for publication: *WinGX* (Farrugia, 2012), *SHELXL2018* (Sheldrick, 2015b), *PLATON* (Spek, 2009) and *pubCIF* (Westrip, 2010).

2-[5-(4-Methylbenzyl)-6-oxo-3-phenyl-1,6-dihydropyridazin-1-yl]acetic acid

Crystal data

$C_{20}H_{18}N_2O_3$

$M_r = 334.36$

Triclinic, $P\bar{1}$

$a = 8.4213$ (7) Å

$b = 9.0739$ (9) Å

$c = 12.2238$ (12) Å

$\alpha = 106.501$ (8)°

$\beta = 92.390$ (8)°

$\gamma = 100.750$ (8)°

$V = 875.43$ (15) Å³

$Z = 2$

$F(000) = 352$

$D_x = 1.268$ Mg m⁻³

Mo $K\alpha$ radiation, $\lambda = 0.71073$ Å

Cell parameters from 9277 reflections

$\theta = 2.4\text{--}30.5^\circ$

$\mu = 0.09$ mm⁻¹

$T = 296$ K

Prism, yellow

$0.75 \times 0.62 \times 0.34$ mm

Data collection

Stoe IPDS 2

diffractometer

Radiation source: sealed X-ray tube, 12 x 0.4

mm long-fine focus

Plane graphite monochromator

Detector resolution: 6.67 pixels mm⁻¹

rotation method scans

Absorption correction: integration

(*X-RED32*; Stoe & Cie, 2002)

$T_{\min} = 0.945$, $T_{\max} = 0.959$

7687 measured reflections

3387 independent reflections

2159 reflections with $I > 2\sigma(I)$

$R_{\text{int}} = 0.029$

$\theta_{\max} = 26.0^\circ$, $\theta_{\min} = 2.5^\circ$

$h = -10 \rightarrow 10$

$k = -10 \rightarrow 11$

$l = -15 \rightarrow 15$

Refinement

Refinement on F^2

Least-squares matrix: full

$R[F^2 > 2\sigma(F^2)] = 0.046$

$wR(F^2) = 0.130$

$S = 1.01$

3387 reflections

228 parameters

33 restraints

Primary atom site location: dual

Secondary atom site location: difference Fourier map
 Hydrogen site location: inferred from neighbouring sites
 H-atom parameters constrained

$$w = 1/[\sigma^2(F_o^2) + (0.0706P)^2]$$

where $P = (F_o^2 + 2F_c^2)/3$
 $(\Delta/\sigma)_{\max} < 0.001$
 $\Delta\rho_{\max} = 0.12 \text{ e } \text{\AA}^{-3}$
 $\Delta\rho_{\min} = -0.14 \text{ e } \text{\AA}^{-3}$

Special details

Geometry. All esds (except the esd in the dihedral angle between two l.s. planes) are estimated using the full covariance matrix. The cell esds are taken into account individually in the estimation of esds in distances, angles and torsion angles; correlations between esds in cell parameters are only used when they are defined by crystal symmetry. An approximate (isotropic) treatment of cell esds is used for estimating esds involving l.s. planes.

Fractional atomic coordinates and isotropic or equivalent isotropic displacement parameters (\AA^2)

	<i>x</i>	<i>y</i>	<i>z</i>	$U_{\text{iso}}^*/U_{\text{eq}}$
O2	0.63260 (15)	1.10394 (16)	0.10937 (10)	0.0735 (4)
H2	0.597450	1.162100	0.078353	0.110*
O3	0.52647 (15)	0.73205 (16)	-0.01452 (10)	0.0764 (4)
O1	0.80943 (17)	1.09371 (19)	-0.02162 (12)	0.0945 (5)
N2	0.68471 (16)	0.84641 (18)	0.15268 (12)	0.0669 (4)
N1	0.72008 (16)	0.88379 (18)	0.26737 (12)	0.0668 (4)
C8	0.46392 (19)	0.7210 (2)	0.26864 (14)	0.0620 (4)
H8	0.389598	0.679405	0.311801	0.074*
C9	0.4288 (2)	0.6836 (2)	0.15452 (14)	0.0620 (4)
C7	0.61225 (19)	0.8228 (2)	0.32473 (14)	0.0613 (4)
C14	0.1506 (2)	0.5207 (2)	0.15768 (15)	0.0664 (4)
C6	0.6544 (2)	0.8672 (2)	0.45037 (15)	0.0680 (5)
C10	0.5447 (2)	0.7524 (2)	0.09055 (14)	0.0634 (4)
C12	0.7494 (2)	1.0492 (2)	0.05303 (14)	0.0670 (5)
C13	0.2753 (2)	0.5779 (2)	0.08692 (16)	0.0734 (5)
H13A	0.226930	0.634241	0.042417	0.088*
H13B	0.303827	0.487485	0.033334	0.088*
C11	0.8048 (2)	0.9243 (3)	0.09364 (17)	0.0773 (5)
H11A	0.830690	0.846172	0.028180	0.093*
H11B	0.903514	0.971292	0.145133	0.093*
C15	0.1700 (3)	0.4072 (2)	0.20852 (19)	0.0832 (6)
H15	0.258956	0.359741	0.194728	0.100*
C19	0.0148 (3)	0.5824 (2)	0.1768 (2)	0.0885 (6)
H19	-0.003886	0.657256	0.142058	0.106*
C17	-0.0729 (3)	0.4267 (3)	0.3010 (2)	0.1019 (7)
C18	-0.0948 (3)	0.5352 (3)	0.2469 (2)	0.1060 (7)
H18	-0.186687	0.578672	0.257801	0.127*
C16	0.0607 (3)	0.3626 (3)	0.2792 (2)	0.0992 (7)
H16	0.078355	0.286573	0.313098	0.119*
C3	0.7361 (4)	0.9592 (4)	0.6852 (2)	0.1101 (9)
H3	0.763972	0.989204	0.763999	0.132*
C1	0.7831 (3)	0.9861 (3)	0.5033 (2)	0.1070 (8)
H1	0.844994	1.038827	0.459306	0.128*
C5	0.5672 (3)	0.7970 (4)	0.51898 (19)	0.1116 (9)

H5	0.478402	0.715558	0.486763	0.134*
C4	0.6081 (3)	0.8448 (5)	0.6369 (2)	0.1338 (11)
H4	0.545236	0.796070	0.682551	0.161*
C2	0.8236 (4)	1.0299 (4)	0.6197 (2)	0.1281 (10)
H2A	0.913185	1.110017	0.653001	0.154*
C20	-0.1911 (4)	0.3793 (4)	0.3811 (3)	0.1591 (13)
H20A	-0.271221	0.443328	0.391357	0.239*
H20B	-0.133254	0.393504	0.453929	0.239*
H20C	-0.243577	0.270862	0.348701	0.239*

Atomic displacement parameters (Å²)

	U^{11}	U^{22}	U^{33}	U^{12}	U^{13}	U^{23}
O2	0.0725 (8)	0.0961 (10)	0.0601 (7)	0.0214 (7)	0.0150 (6)	0.0325 (6)
O3	0.0785 (8)	0.1010 (10)	0.0580 (7)	0.0288 (7)	0.0140 (6)	0.0293 (7)
O1	0.0939 (10)	0.1310 (12)	0.0796 (9)	0.0267 (9)	0.0331 (8)	0.0589 (9)
N2	0.0532 (8)	0.0909 (10)	0.0664 (9)	0.0154 (7)	0.0119 (7)	0.0379 (8)
N1	0.0535 (8)	0.0864 (10)	0.0657 (9)	0.0138 (7)	0.0053 (7)	0.0312 (8)
C8	0.0572 (9)	0.0719 (11)	0.0606 (10)	0.0117 (8)	0.0105 (8)	0.0260 (8)
C9	0.0593 (9)	0.0686 (10)	0.0612 (10)	0.0155 (8)	0.0085 (8)	0.0226 (8)
C7	0.0534 (9)	0.0744 (11)	0.0620 (10)	0.0180 (8)	0.0085 (8)	0.0263 (8)
C14	0.0630 (10)	0.0584 (10)	0.0684 (10)	0.0029 (8)	0.0007 (8)	0.0111 (8)
C6	0.0595 (10)	0.0875 (12)	0.0599 (10)	0.0225 (9)	0.0044 (8)	0.0219 (9)
C10	0.0600 (10)	0.0788 (11)	0.0586 (10)	0.0231 (8)	0.0098 (8)	0.0257 (8)
C12	0.0584 (10)	0.0908 (13)	0.0515 (9)	0.0060 (9)	0.0068 (8)	0.0267 (9)
C13	0.0737 (11)	0.0748 (11)	0.0642 (10)	0.0050 (9)	-0.0002 (9)	0.0165 (9)
C11	0.0556 (9)	0.1085 (15)	0.0800 (12)	0.0164 (10)	0.0190 (9)	0.0462 (11)
C15	0.0817 (13)	0.0735 (12)	0.0977 (14)	0.0177 (10)	0.0199 (11)	0.0284 (11)
C19	0.0741 (13)	0.0770 (13)	0.1100 (17)	0.0140 (10)	0.0034 (12)	0.0228 (12)
C17	0.0866 (14)	0.0909 (14)	0.1061 (16)	-0.0089 (12)	0.0287 (11)	0.0092 (10)
C18	0.0733 (12)	0.1004 (16)	0.1320 (19)	0.0157 (12)	0.0256 (13)	0.0142 (12)
C16	0.1108 (18)	0.0792 (14)	0.1074 (17)	0.0029 (13)	0.0224 (14)	0.0366 (13)
C3	0.1037 (19)	0.164 (3)	0.0617 (13)	0.0585 (19)	0.0004 (14)	0.0139 (16)
C1	0.1183 (19)	0.1081 (17)	0.0751 (14)	-0.0077 (15)	-0.0081 (13)	0.0191 (12)
C5	0.0720 (13)	0.189 (3)	0.0717 (13)	-0.0062 (14)	-0.0022 (11)	0.0583 (15)
C4	0.0910 (17)	0.243 (4)	0.0762 (15)	0.023 (2)	0.0094 (14)	0.068 (2)
C2	0.143 (2)	0.133 (2)	0.0775 (17)	0.0047 (19)	-0.0182 (17)	0.0019 (16)
C20	0.138 (2)	0.158 (3)	0.145 (3)	-0.033 (2)	0.064 (2)	0.022 (2)

Geometric parameters (Å, °)

O2—C12	1.317 (2)	C11—H11B	0.9700
O2—H2	0.8200	C15—C16	1.372 (3)
O3—C10	1.2433 (19)	C15—H15	0.9300
O1—C12	1.193 (2)	C19—C18	1.377 (3)
N2—N1	1.3516 (19)	C19—H19	0.9300
N2—C10	1.370 (2)	C17—C16	1.363 (3)
N2—C11	1.459 (2)	C17—C18	1.367 (4)

N1—C7	1.307 (2)	C17—C20	1.515 (4)
C8—C9	1.344 (2)	C18—H18	0.9300
C8—C7	1.422 (2)	C16—H16	0.9300
C8—H8	0.9300	C3—C2	1.327 (4)
C9—C10	1.438 (2)	C3—C4	1.330 (4)
C9—C13	1.507 (2)	C3—H3	0.9300
C7—C6	1.482 (2)	C1—C2	1.374 (3)
C14—C19	1.365 (3)	C1—H1	0.9300
C14—C15	1.375 (3)	C5—C4	1.390 (3)
C14—C13	1.499 (3)	C5—H5	0.9300
C6—C5	1.352 (3)	C4—H4	0.9300
C6—C1	1.366 (3)	C2—H2A	0.9300
C12—C11	1.498 (3)	C20—H20A	0.9600
C13—H13A	0.9700	C20—H20B	0.9600
C13—H13B	0.9700	C20—H20C	0.9600
C11—H11A	0.9700		
C12—O2—H2	109.5	H11A—C11—H11B	107.7
N1—N2—C10	126.14 (14)	C16—C15—C14	121.4 (2)
N1—N2—C11	115.10 (15)	C16—C15—H15	119.3
C10—N2—C11	118.61 (14)	C14—C15—H15	119.3
C7—N1—N2	117.30 (14)	C14—C19—C18	120.8 (2)
C9—C8—C7	121.38 (16)	C14—C19—H19	119.6
C9—C8—H8	119.3	C18—C19—H19	119.6
C7—C8—H8	119.3	C16—C17—C18	116.7 (2)
C8—C9—C10	117.95 (16)	C16—C17—C20	121.4 (3)
C8—C9—C13	125.62 (16)	C18—C17—C20	121.9 (3)
C10—C9—C13	116.42 (15)	C17—C18—C19	122.2 (2)
N1—C7—C8	121.32 (15)	C17—C18—H18	118.9
N1—C7—C6	115.86 (15)	C19—C18—H18	118.9
C8—C7—C6	122.82 (16)	C17—C16—C15	121.7 (2)
C19—C14—C15	117.17 (19)	C17—C16—H16	119.1
C19—C14—C13	121.17 (18)	C15—C16—H16	119.1
C15—C14—C13	121.63 (17)	C2—C3—C4	119.2 (2)
C5—C6—C1	116.45 (19)	C2—C3—H3	120.4
C5—C6—C7	122.76 (18)	C4—C3—H3	120.4
C1—C6—C7	120.77 (19)	C6—C1—C2	121.7 (3)
O3—C10—N2	119.17 (16)	C6—C1—H1	119.2
O3—C10—C9	124.97 (17)	C2—C1—H1	119.2
N2—C10—C9	115.86 (14)	C6—C5—C4	121.1 (3)
O1—C12—O2	124.94 (17)	C6—C5—H5	119.5
O1—C12—C11	121.98 (17)	C4—C5—H5	119.5
O2—C12—C11	113.06 (14)	C3—C4—C5	120.8 (3)
C14—C13—C9	114.91 (15)	C3—C4—H4	119.6
C14—C13—H13A	108.5	C5—C4—H4	119.6
C9—C13—H13A	108.5	C3—C2—C1	120.7 (3)
C14—C13—H13B	108.5	C3—C2—H2A	119.7
C9—C13—H13B	108.5	C1—C2—H2A	119.7

H13A—C13—H13B	107.5	C17—C20—H20A	109.5
N2—C11—C12	113.59 (14)	C17—C20—H20B	109.5
N2—C11—H11A	108.8	H20A—C20—H20B	109.5
C12—C11—H11A	108.8	C17—C20—H20C	109.5
N2—C11—H11B	108.8	H20A—C20—H20C	109.5
C12—C11—H11B	108.8	H20B—C20—H20C	109.5
C10—N2—N1—C7	1.2 (2)	C10—C9—C13—C14	-174.43 (15)
C11—N2—N1—C7	176.75 (15)	N1—N2—C11—C12	-107.68 (17)
C7—C8—C9—C10	-1.3 (2)	C10—N2—C11—C12	68.2 (2)
C7—C8—C9—C13	-179.66 (16)	O1—C12—C11—N2	-159.10 (18)
N2—N1—C7—C8	0.1 (2)	O2—C12—C11—N2	22.1 (2)
N2—N1—C7—C6	-179.55 (14)	C19—C14—C15—C16	-2.6 (3)
C9—C8—C7—N1	0.0 (3)	C13—C14—C15—C16	175.73 (19)
C9—C8—C7—C6	179.63 (15)	C15—C14—C19—C18	1.8 (3)
N1—C7—C6—C5	-170.3 (2)	C13—C14—C19—C18	-176.5 (2)
C8—C7—C6—C5	10.0 (3)	C16—C17—C18—C19	-2.2 (4)
N1—C7—C6—C1	11.5 (3)	C20—C17—C18—C19	178.0 (2)
C8—C7—C6—C1	-168.13 (19)	C14—C19—C18—C17	0.6 (4)
N1—N2—C10—O3	177.73 (15)	C18—C17—C16—C15	1.4 (4)
C11—N2—C10—O3	2.3 (2)	C20—C17—C16—C15	-178.7 (3)
N1—N2—C10—C9	-2.4 (2)	C14—C15—C16—C17	0.9 (4)
C11—N2—C10—C9	-177.82 (15)	C5—C6—C1—C2	1.2 (4)
C8—C9—C10—O3	-177.84 (16)	C7—C6—C1—C2	179.5 (2)
C13—C9—C10—O3	0.7 (3)	C1—C6—C5—C4	-0.1 (4)
C8—C9—C10—N2	2.3 (2)	C7—C6—C5—C4	-178.3 (2)
C13—C9—C10—N2	-179.12 (15)	C2—C3—C4—C5	1.2 (5)
C19—C14—C13—C9	104.4 (2)	C6—C5—C4—C3	-1.2 (5)
C15—C14—C13—C9	-73.8 (2)	C4—C3—C2—C1	0.0 (5)
C8—C9—C13—C14	4.0 (3)	C6—C1—C2—C3	-1.2 (5)

Hydrogen-bond geometry (\AA , $^\circ$)

$D-H\cdots A$	$D-H$	$H\cdots A$	$D\cdots A$	$D-H\cdots A$
O2—H2 \cdots O3 ⁱ	0.82	1.83	2.6358 (16)	167
C3—H3 \cdots O1 ⁱⁱ	0.93	2.51	3.430 (3)	172

Symmetry codes: (i) $-x+1, -y+2, -z$; (ii) $x, y, z+1$.